Transmission Contingency Analysis Based on Data-Driven Equivalencing of Radial Distribution Networks Considering Uncertainties

KUNJIE TANG [1], (Graduate Student Member, IEEE), **MINGYANG GE**[1], **SHUFENG DONG**[1],
JIANYE CUI[2], **AND XIANG MA**[2]

[1]College of Electrical Engineering, Zhejiang University, Hangzhou 310027, China
[2]State Grid Jinhua Power Supply Company, Jinhua 321017, China

Corresponding author: Shufeng Dong (dongshufeng@zju.edu.cn)

ABSTRACT A transmission contingency analysis (TCA) method based on data-driven equivalencing of radial DN distribution networks is proposed. First, an offline-online-combined data-driven model training method is proposed. The historical data are exploited during offline model training considering the uncertainties of loads and distributed generations to achieve partially prepared root nodal power injection functions, where root nodal voltage magnitudes are taken as arguments. After that, the real-time data of loads and DGs are used to determine all coefficients in these functions. In the proposed TCA, DNs will be equivalent to simplified models by distribution system operators (DSOs) with the data-driven method and the models will be sent to the transmission system operator (TSO). Then, TSO can complete the TCA independently. Numerical experiments show that the proposed TCA approach has similar accuracy and higher efficiency compared with the traditional global-power-flow-based TCA approach. It not only significantly reduces communication time between TSO and DSOs, but also saves calculation times, which may benefit real practice in the coordination operation of transmission-distribution-coupled systems in the future.

INDEX TERMS Data-driven equivalencing, offline-online-combined model training, power flow, transmission contingency analysis, uncertainties.

I. INTRODUCTION

Transmission contingency analysis (TCA) is a fundamental tool for transmission power system operations [1]. The TCA usually consists of contingency selection and contingency evaluation. Contingency selection aims to choose critical contingencies to reduce unnecessary contingency evaluation and enhance the overall efficiency of the TCA. The essence of contingency evaluation is to analyze topology and calculate power flow under given transmission contingencies and activate alarms based on analysis results. Thus, the accuracy of TCA is crucial for system security. Due to the administrative separation, transmission networks (TNs) and distribution networks (DNs) are usually managed by different system operators. TCA is usually processed by transmission system operators (TSOs) independently without interactions with

distribution system operators (DSOs), where TNs are modeled in detail while DNs are equivalent as constant loads [2], [3]. This equivalence will not lead to a large deviation because traditional passive DNs have a small effect on TNs [2], [4]. However, due to the high penetration of distributed generations (DGs), the coupling between TNs and DNs will be significantly enhanced. The variation in the outputs of DGs and other active elements will make active DNs have much larger effect on TN power flow compared with traditional passive DNs [3].

To deal with this challenge, some researchers propose the concept of global TCA (GTCA) considering the effects of DNs on TNs in recent years. Ref. [2] proposes a master-slave-splitting-based (MSS) global power flow method, and later, [5] proposes a GTCA algorithm based on this global power flow method. Ref. [6] also implements GTCA considering the detailed modeling of solar photovoltaics. Considering that a complete GTCA usually involves a large

The associate editor coordinating the review of this manuscript and approving it for publication was Pietro Varilone [].

batch of power flow calculations under given contingencies, the time consumption of solving power flow and the communication delays between TSOs and DSOs significantly influence the overall efficiency of GTCA. Ref. [5] proposes several strategies to accelerate GTCA, including GTCA with DN-concerned contingency selection, DC-model-based GTCA, GTCA using DN equivalencing, etc. DN-concerned contingency selection is an important pre-treatment before analysis, and [7] presents two effective strategies to select critical contingencies. DC-model-based GTCA will accelerate power flow calculation compared, but it may also lead to imprecision. GTCA using DN equivalencing not only accelerates global power flow calculation but also decreases the communication between TSO and DSOs. However, [5] does not give a specific method for DN equivalencing.

Network equivalencing or network reduction is a common approach for static power system applications, such as power flow calculation [8], [9], reliability evaluation [10], system planning [11]. In the TCA, a simple and direct method for reducing a radial DN is to simplify it as a constant load, of which the power injections are equal to the total loads in this DN. However, this method neglects the network losses in DNs and the uncertainties of DGs are not fully considered. If the sensitivity of the power injections to the voltage magnitude of DN root nodes of DNs is relatively small, this equivalent method will not lead to a significant deviation. But if this sensitivity is large, the accuracy cannot be guaranteed. With the advancement of active DNs, many PV-typed DGs exist in DNs, which will significantly enlarge this sensitivity [3]. Therefore, some novel methods for handling this circumstance are needed.

To deal with these challenges, data-driven approaches could be considered. In recent years, data-driven approaches have attracted broad attention in power system analysis and optimization. Reference [12] provides a comprehensive survey covering energy big data analytics and its security. Particularly, it discusses the data-driven schemes in the operation of smart grids. Also, some researchers have introduced data-driven approaches to handle with traditional applications in power system operations, such as state estimation [13], topology or parameter identification [14]–[16], power flow [17], optimal power flow [18], unit commitment [19], etc. However, this important technology has not been utilized in TN-DN coordinated analysis.

Thus, this paper proposes a TCA method based on data-driven equivalencing of radial DNs. The main contribution of this paper is that it

i) proposes a data-driven equivalent method for describing the characteristics of DNs considering the uncertainties of DGs and loads. This equivalent method consists of offline training with historical data and online training with real-time data;

ii) proposes a distributed TCA method based on the proposed data-driven equivalent method. The data exchange between TSO and DSO is designed;
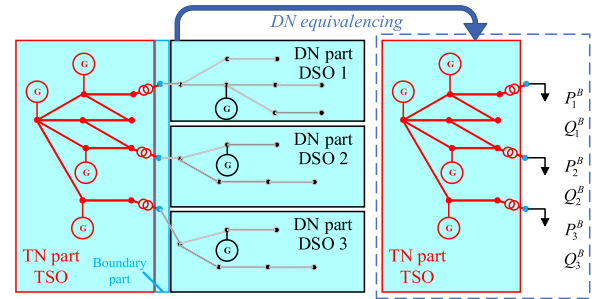

FIGURE 1. DN equivalencing in a TN-DN-coupled system.

iii) proposes several perspectives that should be further addressed when the proposed method is applied to real-world system operations.

Numerical experiments show that the proposed data-driven method can achieve high accuracy. In addition, compared with traditional TCA, the proposed TCA method significantly decreases the communication costs between TSO and DSO, and thus, it has higher efficiency.

The rest of the paper is organized as follows: Section II presents the data-driven equivalencing method of radial DNs. Section III proposes the DN-equivalencing-based TCA method. Numerical experiments demonstrate the effectiveness of the proposed method in Section IV. Discussion and extensions about the proposed method are presented in Section V. Finally, conclusions are drawn in Section VI.

II. DATA-DRIVEN EQUIVALENCING OF RADIAL DNs

This section introduces a data-driven method to establish a DN equivalent model. Subsection A presents the general framework. Subsection B presents some basic assumptions for the proposed method. Subsection C and Subsection D respectively present the offline training part and the online one.

A. GENERAL FRAMEWORK

As mentioned in [5], the influences of DNs are significantly important to achieve accurate TCA results. Global-power-flow-based TCA is presented in this reference. However, a series of global power flow calculation is needed in the TCA. Thus, a large number of alternating iterations between TSO and DSO cost much communication time.

Therefore, the basic idea of this paper is to establish an equivalent model for radial DNs. To be more specific, as shown in FIGURE 1, the power injections are represented as functions of root nodal voltage magnitude of DNs, active and reactive power of loads in DNs, and active and reactive power of DGs in DNs.

$$P^B = f(U^B, \boldsymbol{P}_L^D, \boldsymbol{Q}_L^D, \boldsymbol{P}_G^D, \boldsymbol{Q}_G^D) \tag{1a}$$

$$Q^B = g(U^B, \boldsymbol{P}_L^D, \boldsymbol{Q}_L^D, \boldsymbol{P}_G^D, \boldsymbol{Q}_G^D) \tag{1b}$$

where U^B represents the root nodal voltage magnitude. P^B and Q^B represent active and reactive power injections. $\boldsymbol{P}_L^D$ and $\boldsymbol{Q}_L^D$ represent the active and reactive power of DN loads.
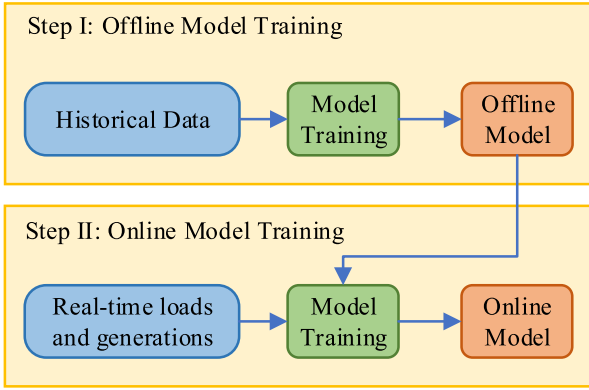
FIGURE 2. General framework of data-driven equivalencing of DNs.

FIGURE 3. Flowchart of offline model training.

P_G^D and Q_G^D represent the active and reactive power of DGs in DNs.

To achieve the functions shown in (1), an offline-online-combined framework is proposed, as shown in FIGURE 2. Two steps are included in this framework. The first step is to train an offline model under a given network topology with historical data. The uncertainties of loads and DGs are considered in this step. The second step is to train an online model under a set of determined loads and generations of DGs, based on the offline model achieved in the first step.

B. BASIC ASSUMPTIONS

With the advancement of DNs, various loads and generations are accessed into DNs. In this paper, without losing generality, some assumptions are established.

i) Flexible loads: the active power and reactive power of DN loads are both modeled as the sum of a forecasted value and a zero-mean fluctuation (normal distribution).

$$\tilde{P}_L^D = P_L^D + \omega_{P_L}^D, \tilde{Q}_L^D = Q_L^D + \omega_{Q_L}^D \qquad (2)$$

where $\omega_{P_L}^D \sim N(0, (\sigma_{P_L}^D)^2)$ and $\omega_{Q_L}^D \sim N(0, (\sigma_{Q_L}^D)^2)$.

ii) DGs: it is assumed that all DGs in DNs are under PQ-typed or PV-typed control. The active power generations of DGs are modeled as an interval.

$$\tilde{P}_G^D \in [P_G^D, \bar{P}_G^D] \qquad (3)$$

Here, if the inverters of DGs are under PV-control, the reactive power of DGs will also vary with random variables. If the inverters of DGs are under PQ-control, it is assumed that the reactive power of DGs remains constant.

iii) The structure of DNs is radial and there are no other active elements in DNs except for the flexible loads and DGs.

C. OFFLINE MODEL TRAINING WITH HISTORICAL DATA

Historical data of loads and generations are used for offline model training by each DSO, as shown in FIGURE 3.

First, for each set of historical data, the relationship between power injections at the root node and root nodal voltage magnitude could be trained. To be more specific, for the t-th set of historical data, $\tilde{P}_{L,t}^D$, $\tilde{Q}_{L,t}^D$, $\tilde{P}_{G,t}^D$, and $\tilde{Q}_{G,t}^D$,
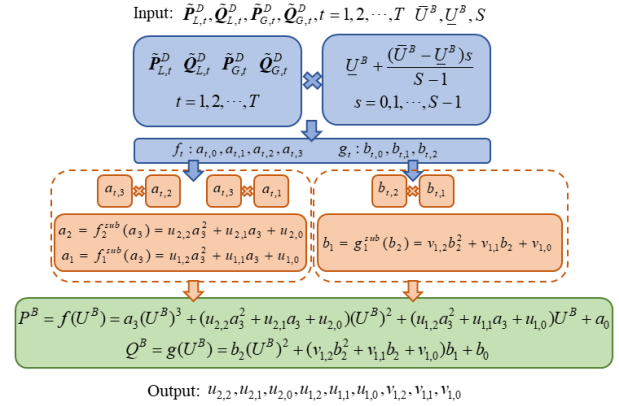
setting different root nodal voltage magnitudes U^B will bring out different power injections P^B and Q^B, f_t and g_t could be achieved with polynomial fitting as shown in (4).

$$P^B = f_t(U^B) = \sum_{i=0}^{n} a_{t,i}(U^B)^i \qquad (4a)$$

$$Q^B = g_t(U^B) = \sum_{i=0}^{m} b_{t,i}(U^B)^i \qquad (4b)$$

where $a_{t,i}$ and $b_{t,i}$ are fitting coefficients. n and m are the order of polynomials. Usually, the higher the order of polynomials is, the more accuracy the fitting is. However, higher order usually requires more data and time to train the model and may also lead to over-fitting problems. According to Bayesian information criterion and a batch of numerical experiments, the setting of $n = 3$ and $m = 2$ is enough to guarantee the accuracy of the fitting, since the correlation coefficient is larger than 0.99 under this setting while $n > 3$ or $m > 2$ will not significantly increase the correlation coefficient. A simple and direct method is to sample U^B uniformly in $[U^B, \bar{U}^B]$, where U^B and $\bar{U}^B$ are the lower and upper limits of U^B. Thus, the sampling points are

$$U^B + \frac{(\bar{U}^B - U^B)s}{S - 1}, \quad s = 0, 1, \cdots, S - 1 \qquad (5)$$

where S is the number of sampling points.

Different sets of loads and generations will bring out different sets of $a_{t,i}$ and $b_{t,i}$. Numerical experiments demonstrate that there is a potential relationship between $a_{t,3}$ and $a_{t,2}$, $a_{t,3}$ and $a_{t,1}$, as well as $b_{t,2}$ and $b_{t,1}$. Thus, as shown in FIGURE 3, f_2^{sub}, f_1^{sub}, and g_1^{sub} can be obtained by the polynomial fitting.

$$a_2 = f_2^{sub}(a_3) = u_{2,2}a_3^2 + u_{2,1}a_3 + u_{2,0} \qquad (6)$$

$$a_1 = f_1^{sub}(a_3) = u_{1,2}a_3^2 + u_{1,1}a_3 + u_{1,0} \qquad (7)$$

$$b_1 = g_1^{sub}(b_2) = v_{1,2}b_2^2 + v_{1,1}b_2 + v_{1,0} \qquad (8)$$

Here, also as shown in FIGURE 3, the final output of offline model training includes $u_{2,2}, u_{2,1}, u_{2,0}, u_{1,2}, u_{1,1}, u_{1,0}$, $v_{1,2}, v_{1,1}, v_{1,0}$, while a_3, a_0, b_2, b_0 are undetermined coefficients, which will be achieved in the online model training.

Input: $u_{2,2}, u_{2,1}, u_{2,0}, u_{1,2}, u_{1,1}, u_{1,0}, v_{1,2}, v_{1,1}, v_{1,0}, \tilde{P}_L^D, \tilde{Q}_L^D, \tilde{P}_G^D, \tilde{Q}_G^D$

Select $U_x^B, U_y^B \in [\underline{U}^B, \bar{U}^B]$

$P_x^B = f(U_x^B), P_y^B = f(U_y^B)$ $Q_x^B = g(U_x^B), Q_y^B = g(U_y^B)$

a_3, a_0 b_2, b_0

$a_2 = u_{2,2}a_3^2 + u_{2,1}a_3 + u_{2,0}$
$a_1 = u_{1,2}a_3^2 + u_{1,1}a_3 + u_{1,0}$ $b_1 = v_{1,2}b_2^2 + v_{1,1}b_2 + v_{1,0}$

$P^B = f(U^B) = a_3(U^B)^3 + a_2(U^B)^2 + a_1 U^B + a_0$
$Q^B = g(U^B) = b_2(U^B)^2 + b_1 U^B + b_0$

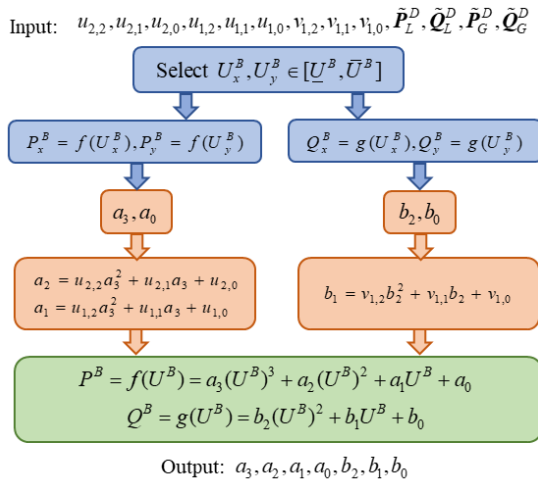Output: $a_3, a_2, a_1, a_0, b_2, b_1, b_0$

FIGURE 4. Flowchart of online model training.

In summary, the uncertainties of loads and generations are included in the historical data. The essence of the offline model training is to achieve 'partially prepared' power injection functions given network topology.

$$P^B = f(U^B) = a_3(U^B)^3 + (u_{2,2}a_3^2 + u_{2,1}a_3 + u_{2,0})(U^B)^2$$
$$+ (u_{1,2}a_3^2 + u_{1,1}a_3 + u_{1,0})U^B + a_0 \quad (9a)$$
$$Q^B = g(U^B) = b_2(U^B)^2 + (v_{1,2}b_2^2 + v_{1,1}b_2 + v_{1,0})b_1 + b_0 \quad (9b)$$

They are generally applicable when the uncertainties satisfy the assumptions presented in Subsection B.

D. ONLINE MODEL TRAINING WITH REAL-TIME DATA

The goal of online model training is to determine the unknown coefficients in (9a) and (9b), i.e. a_3, a_0, b_2, b_0 with the real-time loads and generations. Here, a two-point estimation is applied for online model training. To be more specific, under real-time $\tilde{P}_L^D, \tilde{Q}_L^D, \tilde{P}_G^D, \tilde{Q}_G^D$, take any two different values for U^B, denoted as U_x^B and U_y^B, where $U_x^B, U_y^B \in [\underline{U}^B, \bar{U}^B]$. Calculate DN power flow under U_x^B and U_y^B respectively to achieve

$$P_x^B = f(U_x^B), P_y^B = f(U_y^B) \quad (10a)$$
$$Q_x^B = g(U_x^B), Q_y^B = g(U_y^B) \quad (10b)$$

Then, a_3, a_0, b_2, b_0 could be solved with (10). Note that there are two roots for a_3, a_0, b_2, b_0 since (10a) and (10b) are quadratic equations. Select the appropriate roots as their final solutions. Then, calculate (6)-(8) to achieve other coefficients. Thus, the final DN equivalent model is obtained.

III. DN-EQUIVALENCING-BASED TCA METHOD

This section introduces the DN-equivalencing-based TCA method. Subsection A presents the DN-equivalencing-based power flow method. Then, the overall steps of this TCA method are shown in Subsection B.

A. DN-EQUIVALENCING-BASED POWER FLOW METHOD

Power flow calculation is the basis of TCA. When the online model of DNs is achieved, a DN-equivalencing-based power flow method is as follows.

Step I: Initialize the voltage magnitude of root nodes of DNs U_0^B. Set iteration count $k = 0$ and convergence tolerance ε.

Step II: Calculate boundary power injections P_k^B and Q_k^B with and (1a) and (1b).

Step III: Calculate TN power flow with P_k^B and Q_k^B to achieve U_{k+1}^B.

Step IV: If $\|U_{k+1}^B - U_k^B\| < \varepsilon$, the method converges and stops. Otherwise, let $k = k + 1$ and go back to Step II.

Based on the convergence analysis in [2], the above method can converge if

$$\left| \frac{\partial g}{\partial U^B} \right| \left| \frac{\partial U_T^B}{\partial Q_T^B} \right| < 1 \quad (11)$$

where $\partial U_T^B / \partial Q_T^B$ represents the sensitivity of the DN root nodal voltage magnitude to the reactive power injection at this root node in TN power flow.

B. OVERALL STEPS OF DN-EQUIVALENCING-BASED TCA METHOD

The overall steps of the DN-equivalencing-based TCA method are as follows. Meanwhile, a flowchart of the TCA method is shown in FIGURE 5.

Step I: TSO generates a contingency set and sends a TCA request to all DSOs.

Step II: Each DSO trains its online model with its offline model (corresponding to its current operating mode) as well as the real-time loads and generations of DGs. Then, send the achieve online model to TSO.

Step III: Select a contingency. If this contingency does not lead to a network split, TSO calculates power flow with alternating iterations between the TN model and equivalent models of DNs as shown in Subsection A under this contingency.

Step IV: Check the system security under the selected contingency. If there is a risk (network split, nodal voltage magnitude violation, line overloading, etc.), activate an alarm to operators.

Step V: If the selected contingency is the last one in the contingency set, the TCA method finishes. Otherwise, go back to Step III.

FIGURE 5 shows that the only information exchange occurs at the beginning of the TCA method. To be more specific, TSO only needs to send a TCA request to DSOs, while each DSO only needs to send its online model to the TSO. As shown in Section II, each online model consists of only 7 constants. Thus, compared with traditional GTCA, the proposed TCA method can significantly reduce communication costs between TSO and DSOs. Besides, this feature is important when the communication condition between TSO and DSOs is bad. For example, when communication delay is
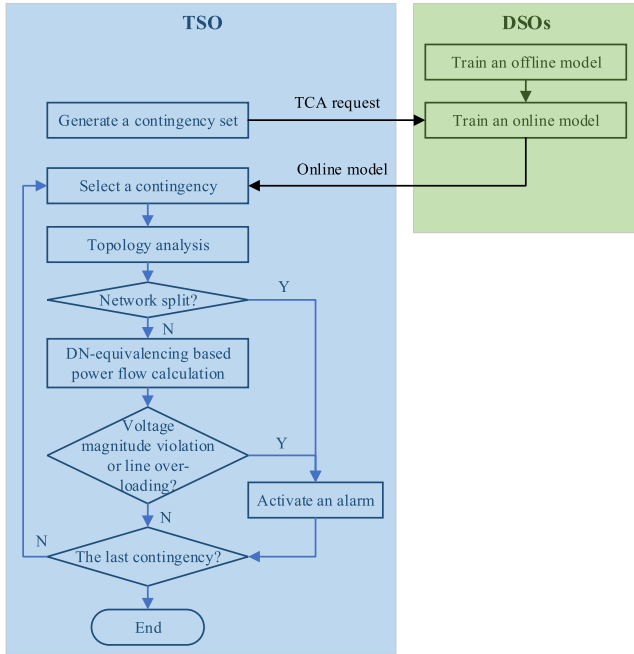
FIGURE 5. Flowchart of DN-equivalencing-based TCA.

FIGURE 6. Curves of power injections v.s root nodal voltage magnitude-Case69.

TABLE 1. Error analysis under uncertainties – modified Case69.

$\tilde{P}_G^D$ /MW	P / Q	Equivalent function	RMSE	MAE
0.5	P /MW	$P^B = -2972.7(U^B)^3 + 579.3(U^B)^2 - 10.8U^B + 2.8$	0.0786	0.2197
	Q /MVar	$Q^B = -290.0(U^B)^2 + 230.7U^B - 2.2$	0.1447	0.4416
1.0	P /MW	$P^B = -2213.9(U^B)^3 + 497.9(U^B)^2 - 3.6U^B + 1.8$	0.0536	0.1691
	Q /MVar	$Q^B = -234.6(U^B)^2 + 224.1U^B - 0.4$	0.1066	0.3172
1.5	P /MW	$P^B = -1840.0(U^B)^3 + 453.4(U^B)^2 + 1.1U^B + 1.1$	0.0433	0.1405
	Q /MVar	$Q^B = -203.9(U^B)^2 + 220.0U^B + 0.8$	0.0879	0.2578
2.0	P /MW	$P^B = -1608.9(U^B)^3 + 424.0(U^B)^2 + 4.4U^B + 0.6$	0.0373	0.1236
	Q /MVar	$Q^B = -183.5(U^B)^2 + 217.1U^B + 1.8$	0.0763	0.2258

TABLE 2. Accuracy and efficiency comparison – case A.

	TCA in this paper		GTCA	
	Contingency	Alarm	Contingency	Alarm
Accuracy	Line #6-#8	#8 (0.86 p.u.)	Line #6-#8	#8 (0.86 p.u.)
	Line #15-#23	Line #23-#24 (16.00MW)	Line #15-#23	Line #23-#24 (16.00MW)
	Line #23-#24	Line #15-#23 (16.00MW)	Line #23-#24	Line #15-#23 (16.00MW)
	Line #27-#29	Line #27-#30 (17.06MW)	Line #27-#29	Line #27-#30 (17.06MW)
	Line #27-#30	Line #27-#29 (17.31MW)	Line #27-#30	Line #27-#29 (17.82MW)
	Part	Time /ms	Part	Time /ms
Efficiency	DSO training	10	TSO calculation	56
	TSO calculation	205	DSO calculation	296
	communication	100	communication	5700
	Total	315	Total	6052

large or non-instantaneous interruptions occur, the traditional GTCA cannot proceed to obtain the final solutions within a proper time.

IV. NUMERICAL EXPERIMENTS
This paper constructs two cases for numerical experiments. The programs are written in MATLAB R2015a and run on the Windows 10 of 64 bits. The CPU is Intel Core i7-7700K, with 4.20GHz master frequency and 32GB memory. The maximum iteration times of the Newton method and the tolerance are set to 50 and 1e-4 p.u., respectively. Set ε = 1e-4 p.u. The historical data are generated with the Monte-Carlo method based on (2) and (3) (sampling size: 1000).

A. CASE A: ONE TSO AND ONE DSO
Case A is constructed by combining a TN case-IEEE Case30 (the lower and upper limits of nodal voltage magnitude are 0.925 p.u. and 1.075 p.u., the active power limits of lines and transformers are set as the values in the 'case30.m' in MATPOWER) with a DN case-modified IEEE Case 69 via a transformer (r = 0.002 p.u., x = 0.01 p.u., ratio = 1.0) at Bus 30. In the DN case, three PV-typed DGs ($\underline{P}_G^D = 0$, $\bar{P}_G^D = 2$MW) are accessed into the DN at Node 8, 15, and 20. Other parameters are $\sigma_{Q_L}^D = 0.05$MVar. $\sigma_{P_L}^D = 0.05$MW. $U^B = 0.925$p.u. $\bar{U}^B = 1.075$p.u. $S = 151$. P_L^D and Q_L^D are set as the values of loads in IEEE Case69.

First, FIGURE 6 compares the DN equivalent curves, achieved by the proposed training method, with the scatter plots, achieved by setting different root nodal voltage magnitudes. The real-time data: $\tilde{P}_G^D = 0.5$MW, $\tilde{P}_L^D = P_L^D$, $\tilde{Q}_L^D = Q_L^D$. It shows that the equivalent curves achieved by the
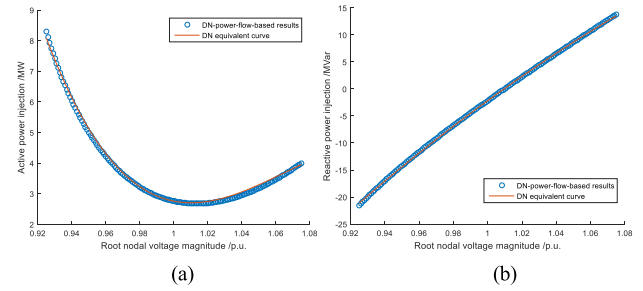
proposed method are very close to the actual characteristics of the DN.

Second, TABLE 1 records the root mean square error (RMSE) and maximum absolute error (MAE) of the achieved DN equivalent curve under different values of $\tilde{P}_G^D$ to evaluate the generality of the proposed training method under uncertainties. It shows that, under different $\tilde{P}_G^D$, the RMSE is less than 0.1MW and 0.2MVar, and the MAE is less than 0.3MW and 0.5MVar. The accuracy is acceptable in TCA. This demonstrates that the DN equivalent function achieved by the proposed offline training method has a good generality under uncertainties.

Third, the accuracy and efficiency of the proposed TCA method and traditional GTCA are compared in TABLE 2. Since offline model training is completed in advance, the cost of this step will not be included in the total time cost of the proposed TCA. The contingency set consists of all N-1 branch-typed contingencies which will not lead to a
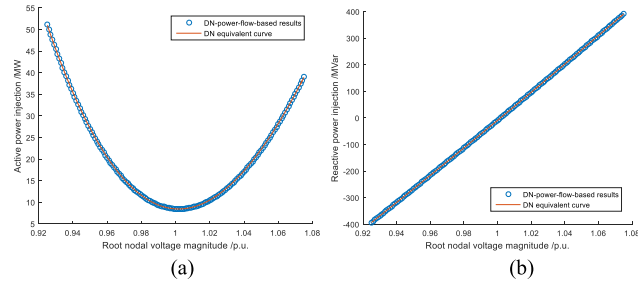
FIGURE 7. Curves of power injections v.s root nodal voltage magnitude-Case141.

network split. The real-time data of DGs: $\tilde{P}_G^D = 0.5$MW. The communication delay between TSO and DSOs is assumed as 50ms.

TABLE 2 shows that the proposed DN-equivalencing-based TCA can achieve almost the same results compared with the traditional GTCA. However, the proposed method has higher efficiency. The GTCA needs 57 alternating iterations between TSO and DSOs. However, the proposed TCA only needs to communicate once (TSO sends a request to DSOs while DSOs send their online models to TSO). The calculation time of the proposed TCA is also less than that of the GTCA, saving over 1/3 of calculation time.

B. CASE B: ONE TSO AND MULTIPLE DSOs

Case B is constructed by combining a TN case-IEEE Case118 (the lower and upper limits of nodal voltage magnitude are 0.925 p.u. and 1.075 p.u.) with four DN case-modified Case 141 via a transformer ($r = 0.002$ p.u., $x = 0.01$ p.u., ratio $= 1.0$) at Bus 35, 45, 75, and 95, respectively. The basic Case141 is shown in the 'case141.m' in MATPOWER. Seven PV-typed DGs ($P_G^D = 0$, $\bar{P}_G^D = 2$MW) are accessed into the DN at Node 8, 15, 20, 47, 68, 45, 61. P_L^D and Q_L^D are set as the values of loads in the 'case141.m' in MATPOWER.

First, similar to FIGURE 6, FIGURE 7 compares the DN equivalent curves with the scatter plots. The real-time data of DGs: $\tilde{P}_G^D = 0.5$MW, $\tilde{P}_L^D = P_L^D$, $\tilde{Q}_L^D = Q_L^D$. It also shows that the DN equivalent curves achieved by the proposed training method are very close to the actual characteristics of the DN.

Second, similar to TABLE 1, TABLE 3 records the RMSE and MAE of the achieved DN equivalent curve under different values of $\tilde{P}_G^D$ to evaluate the generality of the proposed training method under uncertainties. It shows that, under different $\tilde{P}_G^D$, the RMSE is less than 0.2MW and 0.2MVar, and the MAE is less than 0.4MW and 0.4MVar. The accuracy is acceptable in TCA.

FIGURE 6, FIGURE 7, TABLE 1, and TABLE 3 demonstrate that the proposed algorithm can achieve accurate equivalent functions for different DN cases.

Third, similar to TABLE 2, the accuracy and efficiency of the TCA method and traditional GTCA are compared in TABLE 4. The real-time data of DGs in four DNs are: $\tilde{P}_G^{D_1} = 0.5$MW, $\tilde{P}_G^{D_2} = 1$MW, $\tilde{P}_G^{D_3} = 1.5$MW, $\tilde{P}_G^{D_4} = 2$MW. Besides, it is assumed that all DSOs work in a distributed manner.

TABLE 3. Error analysis under uncertainties – modified case141.

$\tilde{P}_G^D$ /MW	P / Q	Equivalent function	RMSE	MAE
0.5	P /MW	$P^B = -10176(U^B)^3 + 6487(U^B)^2 - 23U^B + 8$	0.1130	0.2166
	Q /MVar	$Q^B = 1366.0(U^B)^2 + 5227.0U^B - 8.9$	0.1412	0.3563
1.0	P /MW	$P^B = -9994.4(U^B)^3 + 6440.5(U^B)^2 - 10.5U^B + 4.9$	0.1166	0.2712
	Q /MVar	$Q^B = 1378.6(U^B)^2 + 5223.1U^B - 4.3$	0.1373	0.3763
1.5	P /MW	$P^B = -9818.3(U^B)^3 + 6395.0(U^B)^2 + 1.9U^B + 1.4$	0.1255	0.3220
	Q /MVar	$Q^B = 1391.3(U^B)^2 + 5219.2U^B + 0.2$	0.1353	0.4056
2.0	P /MW	$P^B = -9649.6(U^B)^3 + 6350.9(U^B)^2 + 14.2U^B - 2.1$	0.1373	0.3653
	Q /MVar	$Q^B = 1401.2(U^B)^2 + 5216.2U^B + 4.7$	0.1318	0.3548

TABLE 4. Accuracy and efficiency comparison – case B.

	TCA in this paper		GTCA	
	Contingency	Alarm	Contingency	Alarm
Accu-racy	Line #11-#13	#13 (0.9021 p.u.)	Line #11-#13	#13 (0.9021 p.u.)
	Line #22-#23	#21, #22 (0.9205 p.u., 0.9139 p.u.)	Line #22-#23	#21, #22 (0.9205 p.u., 0.9139 p.u.)
	Line #49-#51	#51, #52 (0.9202 p.u., 0.9189 p.u.)	Line #49-#51	#51, #52 (0.9202 p.u., 0.9189 p.u.)
	Line #51-#52	#52 (0.9118 p.u.)	Line #51-#52	#52 (0.9118 p.u.)
	Line #53-#54	#53 (0.9117 p.u.)	Line #53-#54	#53 (0.9117 p.u.)
	Part	**Time /ms**	**Part**	**Time /ms**
Effi-ciency	DSO training	20	TSO calculation	1043
	TSO calculation	1170	DSO calculation	1041
	communciation	100	communciation	42300
	Total	1290	Total	44384

Similar to TABLE 2, TABLE 4 also shows that the proposed DN-equivalencing-based TCA can achieve almost the same results compared with the traditional GTCA. However, the proposed method has higher efficiency. The GTCA needs 423 alternating iterations between TSO and DSOs. However, the proposed TCA only needs to communicate once and saves over 40s of communication time. Even if communication time is neglected, the calculation time of the proposed TCA is also less than that of the GTCA, saving around 1/3 of calculation time.

TABLE 2 and TABLE 4 show that, when the number of contingencies is large, the traditional GTCA will cost much time on communication, because more contingencies usually indicate more alternating iterations between TSO and DSOs. As a result, the time consumption of the GTCA is extremely sensitive to communication delays On the contrary, in the proposed TCA method, TSO and DSOs only need to exchange information once. Thus, its time consumption is not sensitive to communication delays. In short, the proposed TCA method has significant advantages when communication delay is long or the number of contingencies is large, compared with the GTCA.

V. DISCUSSIONS AND EXTENSIONS
This section discusses some practical issues when the proposed TCA is adopted in real-world operations.

A. CONVERGENCE IMPROVEMENT OF DN-EQUIVALENCING-BASED POWER FLOW METHOD

Similar to the MSS-based power flow method, the proposed DN-equivalencing-based power flow method may diverge if the convergence condition (11) is not satisfied. PV-typed DGs in DNs usually lead to this problem. To deal with this problem, an effective way is to apply the successive-intersection-approximation-based power flow method to improve the convergence of the proposed method. Thus, Step IV in Section III-A is modified as

Step IV': If $\left\| U_{k+1}^B - U_k^B \right\| < \varepsilon$, the method converges and stops.

Step V': Let $k = k + 1$. If k is an even number, update U_k^B

$$U_k^B \leftarrow U_{k-2}^B - \frac{(U_k^B - U_{k-1}^B)^2}{U_k^B - 2U_{k-1}^B + U_{k-2}^B} \quad (12)$$

and go back to Step II.

The convergence will be significantly improved since this method has a local quadratic convergence rate, as demonstrated in [3], while the MSS-based method only has a local linear convergence rate. On the other hand, a sufficient condition for the convergence of the MSS-based method is relaxed in the proof for the convergence of the successive-intersection-approximation-based method [3], so the latter method usually has a broader convergence domain.

B. ACCELERATION OF OFFLINE MODEL TRAINING

Offline model training usually does not have a high real-time requirement. However, if the scale of historical data or the scale of TN is large, offline model training will be very time-consuming. Also, as mentioned above, the proposed offline model training is processed given a topology structure. That is to say, if the switching frequency of the topology structure is relatively high, offline model training should be accelerated to satisfy this requirement. High-performance computing techniques could be adopted in real-world operations, such as GPU-CPU heterogeneous computing, CPU-multithreading computing, fusion cluster [20], etc.

C. CONTINGENCY SELECTION

To further enhance the efficiency of TCA, selecting critical contingencies is necessary. References [5] present some techniques, such as DC-power-flow-based contingency screening, compensation method, global-power-flow-based method, etc, which could be also extended to the TCA proposed in this paper.

D. EXTENSIONS IN DNs WITH LOOPS

Sometimes, the loops exist in DNs, which may significantly influence the global power flow. DNs with loops will make data-driven equivalencing much more difficult since the voltage angle of root nodes should be considered.

Some advanced data-driven techniques may be adopted to deal with this challenge, such as neural network fitting, which will be further discussed in our future work.

VI. CONCLUSION

This paper proposes a TCA method based on data-driven equivalencing of radial DNs. An offline-online-combined approach is proposed to train DN equivalent models. Also, the uncertainties of loads and generations are considered. Through extensive demonstration in many cases, the following observations can be obtained:

- The proposed data-driven equivalent method has a high accuracy, which can satisfy the requirement of the TCA.
- In the proposed data-driven equivalent method, the offline training part can achieve a general relationship under a given topology structure, which can be further trained to obtain accurate DN equivalent functions under different uncertainties. The RMSE of active and reactive power injections are usually less than 0.2MW and 0.2MVar.
- The proposed DN-equivalencing-based TCA method can achieve almost the same results as the traditional GTCA. The more important is, it significantly reduces communication time and saves around 1/3 calculation time.

Some practical issues mentioned in Section V will be further studied in the future. Also, future work will extend data-driven methods to solve other TN-DN coordinated analysis, such as the coordinated optimization of TN-DN-coupled systems.

REFERENCES

[1] M. Shahidehpour, F. Tinney, and Y. Fu, "Impact of security on power systems operation," *Proc. IEEE*, vol. 93, no. 11, pp. 2013–2025, Nov. 2005, doi: 10.1109/JPROC.2005.857490.

[2] H. Sun, Q. Guo, B. Zhang, Y. Guo, Z. Li, and J. Wang, "Master–slave-splitting based distributed global power flow method for integrated transmission and distribution analysis," *IEEE Trans. Smart Grid*, vol. 6, no. 3, pp. 1484–1492, May 2015, doi: 10.1109/TSG.2014.2336810.

[3] K. Tang, S. Dong, and Y. Song, "Successive-intersection-approximation-based power flow method for integrated transmission and distribution networks," *IEEE Trans. Power Syst.*, vol. 35, no. 6, pp. 4836–4846, Nov. 2020, doi: 10.1109/TPWRS.2020.2994312.

[4] Z. Li, H. Sun, Q. Guo, J. Wang, and G. Liu, "Generalized master–slave-splitting method and application to transmission–distribution coordinated energy management," *IEEE Trans. Power Syst.*, vol. 34, no. 6, pp. 5169–5183, Nov. 2019, doi: 10.1109/TPWRS.2018.2890169.

[5] Z. Li, J. Wang, H. Sun, and Q. Guo, "Transmission contingency analysis based on integrated transmission and distribution power flow in smart grid," *IEEE Trans. Power Syst.*, vol. 30, no. 6, pp. 3356–3367, Nov. 2015, doi: 10.1109/TPWRS.2014.2381879.

[6] M. Gupta and A. R. Abhyankar, "Impact of active distribution network on contingency analysis of transmission system," in *Proc. North Amer. Power Symp. (NAPS)*, Oct. 2019, pp. 1–6, doi: 10.1109/NAPS46351.2019.9000317.

[7] Z. Li, J. Wang, H. Sun, and Q. Guo, "Transmission contingency screening considering impacts of distribution grids," *IEEE Trans. Power Syst.*, vol. 31, no. 2, pp. 1659–1660, Mar. 2016, doi: 10.1109/TPWRS.2015.2412692.

[8] Y. Zhang, M. Larsson, J. Turunen, and L. Haarla, "Network reduction for power flow based applications," in *Proc. IEEE Grenoble Conf.*, Jun. 2013, pp. 1–6, doi: 10.1109/PTC.2013.6652445.

[9] X. Cheng and T. J. Overbye, "PTDF-based power system equivalents," *IEEE Trans. Power Syst.*, vol. 20, no. 4, pp. 1868–1876, Nov. 2005, doi: 10.1109/TPWRS.2005.857013.

[10] S. Wang, Y. Ding, C. Ye, C. Wan, and Y. Mo, "Reliability evaluation of integrated electricity–gas system utilizing network equivalent and integrated optimal power flow techniques," *J. Modern Power Syst. Clean Energy*, vol. 7, no. 6, pp. 1523–1535, Nov. 2019, doi: 10.1007/s40565-019-0566-x.

[11] H. Oh, "A new network reduction methodology for power system planning studies," *IEEE Trans. Power Syst.*, vol. 25, no. 2, pp. 677–684, May 2010.

[12] J. Hu and A. V. Vasilakos, "Energy big data analytics and security: Challenges and opportunities," *IEEE Trans. Smart Grid*, vol. 7, no. 5, pp. 2432–2436, May 2016, doi: 10.1109/TSG.2016.2563461.

[13] A. Monticelli, "Electric power system state estimation," *Proc. IEEE*, vol. 88, no. 2, pp. 262–282, Feb. 2000, doi: 10.1109/5.824004.

[14] J. Yu, Y. Weng, and R. Rajagopal, "PaToPa: A data-driven parameter and topology joint estimation framework in distribution grids," *IEEE Trans. Power Syst.*, vol. 33, no. 4, pp. 4335–4347, Jul. 2018, doi: 10.1109/TPWRS.2017.2778194.

[15] D. Deka, S. Backhaus, and M. Chertkov, "Structure learning in power distribution networks," *IEEE Trans. Control Netw. Syst.*, vol. 5, no. 3, pp. 1061–1074, Sep. 2018, doi: 10.1109/TCNS.2017.2673546.

[16] S. Jayadev Pappu, N. Bhatt, R. Pasumarthy, and A. Rajeswaran, "Identifying topology of low voltage distribution networks based on smart meter data," *IEEE Trans. Smart Grid*, vol. 9, no. 5, pp. 5113–5122, Sep. 2018, doi: 10.1109/TSG.2017.2680542.

[17] J. Yu, Y. Weng, and R. Rajagopal, "Robust mapping rule estimation for power flow analysis in distribution grids," in *Proc. North Amer. Power Symp. NAPS*, Sep. 2017, pp. 1–6, doi: 10.1109/NAPS.2017.8107397.

[18] T. Ding, Q. Yang, Y. Yang, C. Li, Z. Bie, and F. Blaabjerg, "A data-driven stochastic reactive power optimization considering uncertainties in active distribution networks and decomposition method," *IEEE Trans. Smart Grid*, vol. 9, no. 5, pp. 4994–5004, Sep. 2018, doi: 10.1109/TSG.2017.2677481.

[19] Z. J. Lin, H. Chen, and X. Yin, "Data-driven stochastic unit commitment for integrating wind generation," *IEEE Trans. Power Syst.*, vol. 34, no. 5, p. 3983, Sep. 2019, doi: 10.1109/TPWRS.2019.2932510.

[20] X. Yang, C. Liu, and J. Wang, "Large-scale branch contingency analysis through master/slave parallel computing," *J. Mod. Power Syst. Clean Energy*, vol. 1, no. 2, pp. 159–166, 2013, doi: 10.1007/s40565-013-0024-0.

MINGYANG GE was born in Changchun, Jilin, China, in 1999. He received the bachelor's degree from Zhejiang University, Hangzhou, China, where he is currently pursuing the Ph.D. degree.

SHUFENG DONG received the B.E. and Ph.D. degrees from Tsinghua University, Beijing, China, in 2004 and 2009, respectively. He is currently an Assistant Professor and a Qiushi Young Scholar with the College of Electrical Engineering, Zhejiang University, Hangzhou, China. His research interests include power system state estimation, cloud computing, and high-performance computing in power systems.

JIANYE CUI is currently a Senior Engineer with State Grid Jinhua Power Supply Company, Jinhua, China. His research interest includes power system automation.

KUNJIE TANG (Graduate Student Member, IEEE) received the B.E. degree from the College of Electrical Engineering, Zhejiang University, Hangzhou, China, in 2017, where he is currently pursuing the Ph.D. degree. His research interests include transmission-distribution coordinated optimization and high-performance computing in power systems.

XIANG MA is currently a Senior Engineer with State Grid Jinhua Power Supply Company, Jinhua, China. His research interest includes power system automation.

• • •